

A Comparative Theoretical-Experimental Analysis of a Video Reflectometry Setup

ABSTRACT

Video Reflectometry is a relatively simple technique to determine of the optical properties of biological tissues. The video image captures the spatially resolved diffuse reflectance, $Rd(r)$, generated by a narrow light beam normally incident on the surface of the tissue. The video system uses a CCD camera in combination with optical density filters that allows recording of the reflectance signal over a large dynamic range. In this paper, we describe the theoretical framework for evaluating experimental measurements using Monte Carlo simulations. The influence of various factors on the derived optical properties is presented. The specific factors explored are (1) mis-focusing of the camera on the surface, (2) tilting of incident beam, (3) finite beam diameter. Finally, we present experimental results of the performance of the system on using Teflon disks as optical standards.

M. Cunill Rodríguez^a, José A. Delgado^a, Sergio Vázquez^a, Beatriz Morales^a, Scott A. Prah^b, Jorge Castro^a

a) Instituto Nacional de Astrofísica, Óptica y Electrónica (INAOE), Puebla, México.
b) Oregon Medical Laser Center, Providence St. Vincent Medical Center, 9205 S.W., Barnes Rd Portland OR 97225, USA.

Introduction

Video reflectometry

Is a technique to obtain information of the optical parameters (OP) of biological tissues from the study of the radial distribution of the light in combination with the use the dipole model proposed by Farrell et al. [3] based on the diffusion approximation. In this model, the tissue must be considered homogeneous and semi-infinite, and the reduced scattering coefficient must be much greater than the absorption coefficient.

In this work

- Current investigation involved studying the influence of various factors on the radially resolved diffuse reflectance curve and the implications of these results for the derived optical properties.
- The performance of the system on using Teflon disks as optical standards for to calibrate our set-up.

Materials & Methods

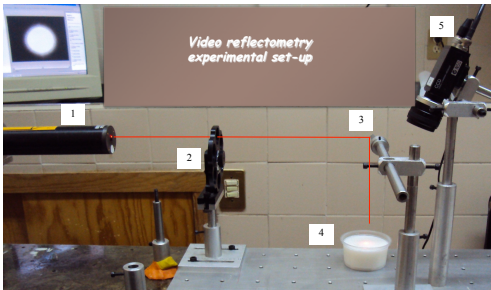


FIGURE 1. A photograph of our video reflectometry experimental set-up 1) 632 nm He-Ne laser, 2) rotatory wheel assembly containing the five neutral density filters, 3) flat mirror, 4) liquid phantom, and 5) CCD camera for detection.

2.1 Mis-focusing of the camera on the surface

A liquid phantom of 20 ml of Lipofundin-10% [8] was deposited into one plastic container, and the distilled water was added until the mixture was leveled up to 112 ml. The phantom was placed over a mounting platform (THORLABS LJ750). The focusing lens was tuned onto the sample surface until the best image was observed on the screen of the PC. Under this focusing conditions the height of the platform was considered as a reference plane, and the images were recorded in this position. Then the position of the phantoms surface was incremented 1.0 mm or decremented 1.0 mm with respect to the reference, taking the correspondent images for each these positions.

2.2 Tilting of incident beam

The fundamental difference between normal and oblique incidence is a shift in the positions of the point sources in the x direction (Fig. 2). The modified dipole source diffusion theory model gives the diffuse reflectance [wang]:

$$Rd(r) = a' (1 - R_s) \frac{1}{4\pi} \left[\frac{z_0 \cos \alpha_t (1 + \mu_{eff} \rho_1) e^{-\mu_{eff} \rho_1}}{\rho_1^3} + \frac{(z_0 \cos \alpha_t + 4AD) (1 + \mu_{eff} \rho_2) e^{-\mu_{eff} \rho_2}}{\rho_2^3} \right] \quad (1)$$

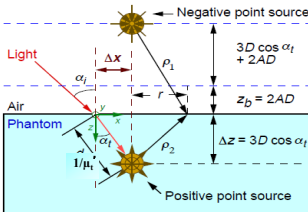


FIGURE 2. Schematic representation of obliquely incident light. Taken from the G. Marquez and L. Wang (1997)

In this study the radially resolved diffuse reflectance was simulated for a tilting of 5° of incident beam, by the equation (1).

- Teflon disks as optical standards

The radial reflectance profiles from experiment and Farrell model are not on the same scale. A reference sample of TEFLON was chosen as optical standard to calibrate the experimental set-up. The scaling factor was determined using a least-squares fitting procedure from a specified radial distance r_0 .

2.3 Finite beam diameter

Our light source is a HE-Ne laser (JDSU, 1144P) which beam diameter is 0.7 mm. A typical He-Ne laser operating in TEM₀₀ mode has a Gaussian profile, which beam diameter is defined as the diameter where the beam's intensity has decreased to 1/e² or 13.5% of its value maximum. In this study the spatially resolved reflectance profiles were obtained for an infinitely small beam and Gaussian beam with diameter $\phi=1$ mm through Monte Carlo (MC) simulations.

References

- Farrell, T. J., M. S. Patterson, and B. C. Wilson, "A diffusion theory model of spatially-resolved, steady-state diffuse reflectance for the non-invasive determination of tissue optical properties in vivo." *Med. Phys.* 19, 879-888 (1992).
- Press, W.H., Teukolsky, S.A., Vetterling, W.T., Flannery, and B. C. Wilson, "Numerical recipes in C: The art of scientific computing" *Med. Phys.* 19, 879-888 (1992).

Results and Discussions

3.1 Mis-focusing of the camera on the surface

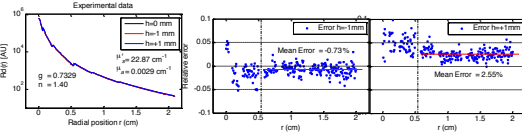


FIGURE 3. Difference between the reflectance curves $Rd(r)$ and $Rd(r)$ with respect to $Rd(r)$. The symbol $\mu_{s,0}$ accompanying $Rd(r)$ indicates the radially resolved reflectance recorded when the position of the phantom surface was incremented 1mm (denoted as $h=+1$ mm) or decremented 1mm (denoted as $h=-1$ mm) with respect to the reference plane $h=0$, respectively.

3.2 Tilting of incident beam

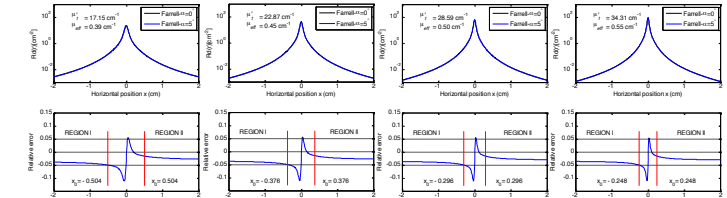


FIGURE 5. Difference between the reflectance curve $Rd(x)$ for $\alpha=5^\circ$ with respect to $Rd(x)$ for the normal incident beam ($\alpha=0^\circ$) for a set of four values of the reduced scattering coefficient μ_s .

3.3 Finite beam diameter

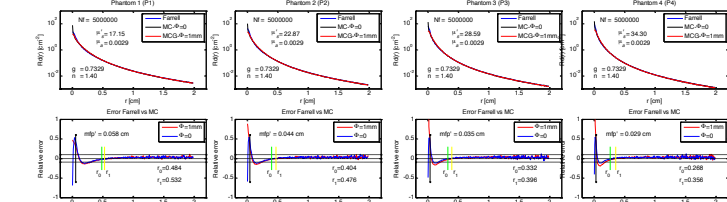
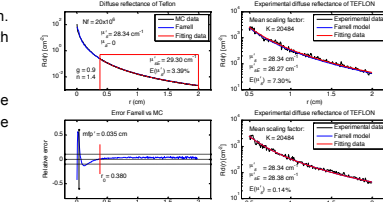


FIGURE 6. Comparison of radially resolved reflectance obtained by Farrell diffusion model, infinitely small beam, and Gaussian beam with $\phi=1$ mm, both simulated with Monte Carlo. It shows the relative error of Farrell with respect to Monte Carlo simulations. The optical properties are shown inside the figure for each phantoms (P1-P4).

-Teflon disks as optical standards



In the left figure shows the radially resolved diffuse reflectance of TEFLON computed with the Monte Carlo model for the optical parameters shows inside the figure. Also, within this same figure shows the results from fitting the Farrell model to Monte Carlo data from the radial position r_0 , where the relative error of the Farrell model with respect to Monte Carlo data is closer to zero while achieving the maximum value at a radial distance equal to transport scattering mean free path (mpf) of tissue. The right figures are the results from fitting the Farrell model to the experimental reflectance data of TEFLON from the radial position 0.494 cm. We only show two of the ten measurements realized (see table 3), the worst and best, respectively. The extracted optical parameter, μ_s , the mean scaling factor K_s , and the relative error expressed in percent, are show within each figure.

TABLES

Table 1. Extracted Optical Properties (OP) from fitting the Farrell model to simulated data with the modified dipole source diffusion theory, for the tilting (5°) of incident beam, in two spatial regions (as shown in figure 5).

Extracted OP (cm ⁻¹)		ERROR (%)	
REGION I	REGION II	REGION I	REGION II
K_s	μ_s	μ_s	μ_s
18.49	0.3205	17.67	0.3839
7.81	14.74	0.0020	31.03
3.03	1.56	0.0028	3.45
24.34	0.4088	23.54	0.4459
6.43	6.16	0.0023	20.89
2.93	0.91	0.0028	3.45
30.22	0.4699	29.47	0.4950
5.7	6.02	0.0024	17.24
3.08	1.00	0.0028	3.45
36.12	0.5223	35.41	0.5390
5.28	5.04	0.0025	13.70
3.21	2.55	0.0027	6.90

Table 2. Extracted Optical Properties from fitting the Farrell model to Monte Carlo data for the finite beam diameter (Gaussian beam) and infinitely small beam.

Extracted Optical Properties (cm ⁻¹)		ERROR (%)	
Infinitely small beam	Gaussian beam	Infinitely small beam	Gaussian beam with diameter $\phi=1$ mm
μ_s	μ_s	μ_s	μ_s
17.25	0.4284	17.24	0.4322
0.58	6.33	0.0016	16.67
0.52	10.82	0.0036	20.00
23.21	0.4694	23.03	0.492
1.49	4.31	0.0032	6.67
0.70	9.33	0.0035	16.67
28.85	0.5399	28.67	0.5537
1.26	7.98	0.0034	13.33
0.28	10.74	0.0036	20.00
34.63	0.5868	34.59	0.5887
0.93	7.02	0.0033	10.00
0.82	7.04	0.0033	10.00

Table 3. Extracted Optical Property (PO) from fitting the Farrell model to TEFLON experimental data in 10 measurement realized. This PO was extracted by two form; with each value of the scaling factor (K_s), and with the mean scaling factor (K_m). Fitting Errors for μ_s at two forms.

Scaling Factor K_s	Extracted OP μ_s (cm ⁻¹)	Error (%)	Extracted OP with the mean Scaling Factor K_m	Error (%)
19916	27.29	3.71	28.77	1.52
20532	26.96	4.87	26.27	7.30
21043	28.13	6.74	27.76	2.05
22711	30.91	9.07	27.17	4.13
20750	28.84	1.76	28.38	0.14
19854	26.97	4.83	27.98	1.27
21983	27.92	1.48	26.54	6.35
19289	26.53	6.39	28.56	0.78
20220	27.71	2.22	28.09	0.88
18922	25.87	9.42	28.16	0.64
$K_m=20484$	27.69	4.46	27.77	2.81

Conclusions

- We investigated the inverse problem in diffuse reflectance spectroscopy based on the a combination of a simplified diffusion approximation model of human skin and a fiber optic probe configuration with the well known non-linear fitting algorithm of Levenberg-Marquardt.
- It has been shown that our extraction program, based on DA and a non-linear LS fitting method, can be used to recover physiological parameters with accuracy within 5% for f_{bl} , A_s and S . However recovery error values for f_w are above 14% when the synthetic spectra are noise free.
- Retrieval errors for f_w can be minimized using physiological information of this parameter